

Search for the Flavor-Changing Neutral Current Decay

$$D^0 \rightarrow \mu^+ \mu^- \text{ in } p\bar{p} \text{ Collisions at } \sqrt{s}=1.96 \text{ TeV}$$

D. Acosta,¹⁴ T. Affolder,⁷ M.H. Ahn,²⁵ T. Akimoto,⁵² M.G. Albrow,¹³ D. Ambrose,⁴⁰ D. Amidei,³⁰ A. Anastassov,⁴⁷ K. Anikeev,²⁹ A. Annovi,⁴¹ J. Antos,¹ M. Aoki,⁵² G. Apolinari,¹³ J-F. Arguin,⁵⁰ T. Arisawa,⁵⁴ A. Artikov,¹¹ T. Asakawa,⁵² W. Ashmanskas,² A. Attal,⁶ F. Azfar,³⁸ P. Azzi-Bacchetta,³⁹ N. Bacchetta,³⁹ H. Bachacou,²⁶ W. Badgett,¹³ S. Bailey,¹⁸ A. Barbaro-Galtieri,²⁶ G. Barker,²³ V.E. Barnes,⁴³ B.A. Barnett,²² S. Baroiant,⁵ M. Barone,¹⁵ G. Bauer,²⁹ F. Bedeschi,⁴¹ S. Behari,²² S. Belforte,⁵¹ W.H. Bell,¹⁷ G. Bellettini,⁴¹ J. Bellinger,⁵⁵ D. Benjamin,¹² A. Beretvas,¹³ A. Bhatti,⁴⁵ M. Binkley,¹³ D. Bisello,³⁹ M. Bishai,¹³ R.E. Blair,² C. Blocker,⁴ K. Bloom,³⁰ B. Blumenfeld,²² A. Bocci,⁴⁵ A. Bodek,⁴⁴ G. Bolla,⁴³ A. Bolshov,²⁹ P.S.L. Booth,²⁷ D. Bortoletto,⁴³ J. Boudreau,⁴² S. Bourov,¹³ C. Bromberg,³¹ M. Brozovic,¹² E. Brubaker,²⁶ J. Budagov,¹¹ H.S. Budd,⁴⁴ K. Burkett,¹⁸ G. Busetto,³⁹ P. Bussey,¹⁷ K.L. Byrum,² S. Cabrera,¹² P. Calafiura,²⁶ M. Campanelli,¹⁶ M. Campbell,³⁰ A. Canepa,⁴³ D. Carlsmith,⁵⁵ S. Carron,¹² R. Carosi,⁴¹ M. Casarsa,⁵¹ W. Caskey,⁵ A. Castro,³ P. Catastini,⁴¹ D. Cauz,⁵¹ A. Cerri,²⁶ C. Cerri,⁴¹ L. Cerrito,²¹ J. Chapman,³⁰ C. Chen,⁴⁰ Y.C. Chen,¹ M. Chertok,⁵ G. Chiarelli,⁴¹ G. Chlachidze,¹¹ F. Chlebana,¹³ K. Cho,²⁵ D. Chokheli,¹¹ M.L. Chu,¹ J.Y. Chung,³⁵ W-H. Chung,⁵⁵ Y.S. Chung,⁴⁴ C.I. Ciobanu,²¹ M.A. Ciocci,⁴¹ A.G. Clark,¹⁶ M.N. Coca,⁴⁴ A. Connolly,²⁶ M.E. Convery,⁴⁵ J. Conway,⁴⁷ M. Cordelli,¹⁵ G. Cortiana,³⁹ J. Cranshaw,⁴⁹ R. Culbertson,¹³ C. Currat,²⁶ D. Cyr,⁵⁵ D. Dagenhart,⁴ S. DaRonco,³⁹ S. D'Auria,¹⁷ P. de Barbaro,⁴⁴ S. De Cecco,⁴⁶ S. Dell'Agnello,¹⁵ M. Dell'Orso,⁴¹ S. Demers,⁴⁴ L. Demortier,⁴⁵ M. Deninno,³ D. De Pedis,⁴⁶ P.F. Derwent,¹³ C. Dionisi,⁴⁶ J.R. Dittmann,¹³ P. Doksus,²¹ A. Dominguez,²⁶ S. Donati,⁴¹ M. D'Onofrio,¹⁶ T. Dorigo,³⁹ V. Drollinger,³³ K. Ebina,⁵⁴ N. Eddy,²¹ R. Ely,²⁶ R. Erbacher,¹³ M. Erdmann,²³ D. Errede,²¹ S. Errede,²¹ R. Eusebi,⁴⁴ H-C. Fang,²⁶ S. Farrington,¹⁷ I. Fedorko,⁴¹ R.G. Feild,⁵⁶ M. Feindt,²³ J.P. Fernandez,⁴³ C. Ferretti,³⁰ R.D. Field,¹⁴ I. Fiori,⁴¹ G. Flanagan,³¹ B. Flaugh,¹³ L.R. Flores-Castillo,⁴² A. Foland,¹⁸ S. Forrester,⁵ G.W. Foster,¹³ M. Franklin,¹⁸ H. Frisch,¹⁰ Y. Fujii,²⁴ I. Furic,²⁹ A. Gallas,³⁴ M. Gallinaro,⁴⁵ J. Galyardt,⁹ M. Garcia-Sciveres,²⁶ A.F. Garfinkel,⁴³ C. Gay,⁵⁶ H. Gerberich,¹² E. Gerchtein,⁹ D.W. Gerdes,³⁰ S. Giagu,⁴⁶ P. Giannetti,⁴¹ A. Gibson,²⁶ K. Gibson,⁹ C. Ginsburg,⁵⁵ K. Giolo,⁴³ M. Giordani,⁵ G. Giurgiu,⁹

V. Glagolev,¹¹ D. Glenzinski,¹³ M. Gold,³³ N. Goldschmidt,³⁰ D. Goldstein,⁶ J. Goldstein,¹³
G. Gomez,⁸ G. Gomez-Ceballos,²⁹ M. Goncharov,⁴⁸ I. Gorelov,³³ A.T. Goshaw,¹²
Y. Gotra,⁴² K. Goulianatos,⁴⁵ A. Gresele,³ G. Grim,⁵ C. Grossos-Pilcher,¹⁰ M. Guenther,⁴³
J. Guimaraes da Costa,¹⁸ C. Haber,²⁶ K. Hahn,⁴⁰ S.R. Hahn,¹³ E. Halkiadakis,⁴⁴ C. Hall,¹⁸
R. Handler,⁵⁵ F. Happacher,¹⁵ K. Hara,⁵² M. Hare,⁵³ R.F. Harr,³⁰ R.M. Harris,¹³
F. Hartmann,²³ K. Hatakeyama,⁴⁵ J. Hauser,⁶ C. Hays,¹² E. Heider,⁵³ B. Heinemann,²⁷
J. Heinrich,⁴⁰ M. Hennecke,²³ M. Herndon,²² C. Hill,⁷ D. Hirschbuehl,²³ A. Hocker,⁴⁴
K.D. Hoffman,¹⁰ A. Holloway,¹⁸ S. Hou,¹ M.A. Houlden,²⁷ B.T. Huffman,³⁸ R.E. Hughes,³⁵
J. Huston,³¹ K. Ikado,⁵⁴ J. Incandela,⁷ G. Introzzi,⁴¹ M. Iori,⁴⁶ Y. Ishizawa,⁵² C. Issever,⁷
A. Ivanov,⁴⁴ Y. Iwata,²⁰ B. Iyutin,²⁹ E. James,³⁰ D. Jang,⁴⁷ J. Jarrell,³³ D. Jeans,⁴⁶
H. Jensen,¹³ M. Jones,⁴⁰ S.Y. Jun,⁹ T. Junk,²¹ T. Kamon,⁴⁸ J. Kang,³⁰ M. Karagoz Unel,³⁴
P.E. Karchin,³⁰ S. Kartal,¹³ Y. Kato,³⁷ Y. Kemp,²³ R. Kephart,¹³ U. Kerzel,²³ D. Khazins,¹²
V. Khotilovich,⁴⁸ B. Kilminster,⁴⁴ B.J. Kim,²⁵ D.H. Kim,²⁵ H.S. Kim,²¹ J.E. Kim,²⁵
M.J. Kim,⁹ M.S. Kim,²⁵ S.B. Kim,²⁵ S.H. Kim,⁵² T.H. Kim,²⁹ Y.K. Kim,¹⁰ B.T. King,²⁷
M. Kirby,¹² M. Kirk,⁴ L. Kirsch,⁴ S. Klimenko,¹⁴ B. Knuteson,¹⁰ H. Kobayashi,⁵² P. Koehn,³⁵
K. Kondo,⁵⁴ J. Konigsberg,¹⁴ K. Kordas,⁵⁰ A. Korn,²⁹ A. Korytov,¹⁴ K. Kotelnikov,³²
A.V. Kotwal,¹² A. Kovalev,⁴⁰ J. Kraus,²¹ I. Kravchenko,²⁹ A. Kreymer,¹³ J. Kroll,⁴⁰
M. Kruse,¹² V. Krutelyov,⁴⁸ S.E. Kuhlmann,² N. Kuznetsova,¹³ A.T. Laasanen,⁴³ S. Lai,⁵⁰
S. Lami,⁴⁵ S. Lammel,¹³ J. Lancaster,¹² M. Lancaster,²⁸ R. Lander,⁵ K. Lannon,²¹
A. Lath,⁴⁷ G. Latino,³³ R. Lauhakangas,¹⁹ I. Lazzizzera,³⁹ Y. Le,²² C. Lecci,²³
T. LeCompte,² J. Lee,²⁵ J. Lee,⁴⁴ S.W. Lee,⁴⁸ N. Leonardo,²⁹ S. Leone,⁴¹ J.D. Lewis,¹³
K. Li,⁵⁶ C.S. Lin,¹³ M. Lindgren,⁶ T.M. Liss,²¹ D.O. Litvintsev,¹³ T. Liu,¹³ Y. Liu,¹⁶
N.S. Lockyer,⁴⁰ A. Loginov,³² J. Loken,³⁸ M. Loreti,³⁹ P. Loverre,⁴⁶ D. Lucchesi,³⁹
P. Lukens,¹³ L. Lyons,³⁸ J. Lys,²⁶ D. MacQueen,⁵⁰ R. Madrak,¹⁸ K. Maeshima,¹³
P. Maksimovic,²² L. Malferrari,³ G. Manca,³⁸ R. Marginean,³⁵ A. Martin,⁵⁶ M. Martin,²²
V. Martin,³⁴ M. Martinez,¹³ T. Maruyama,¹⁰ H. Matsunaga,⁵² M. Mattson,³⁰ P. Mazzanti,³
K.S. McFarland,⁴⁴ D. McGivern,²⁸ P.M. McIntyre,⁴⁸ P. McNamara,⁴⁷ R. McNulty,²⁷
S. Menzemer,²³ A. Menzione,⁴¹ P. Merkel,¹³ C. Mesropian,⁴⁵ A. Messina,⁴⁶ A. Meyer,¹³
T. Miao,¹³ L. Miller,¹⁸ R. Miller,³¹ J.S. Miller,³⁰ R. Miquel,²⁶ S. Miscetti,¹⁵ M. Mishina,¹³
G. Mitselmakher,¹⁴ A. Miyamoto,²⁴ Y. Miyazaki,³⁷ N. Moggi,³ R. Moore,¹³ M. Morello,⁴¹
T. Moulik,⁴³ A. Mukherjee,¹³ M. Mulhearn,²⁹ T. Muller,²³ R. Mumford,²² A. Munar,⁴⁰
P. Murat,¹³ S. Murgia,³¹ J. Nachtman,¹³ S. Nahm,⁵⁶ I. Nakamura,⁴⁰ I. Nakano,³⁶ A. Napier,⁵³

R. Napora,²² V. Necula,¹⁴ F. Niell,³⁰ J. Nielsen,²⁶ C. Nelson,¹³ T. Nelson,¹³ C. Neu,³⁵ M.S. Neubauer,²⁹ C. Newman-Holmes,¹³ A-S. Nicollerat,¹⁶ T. Nigmanov,⁴² H. Niu,⁴ L. Nodulman,² K. Oesterberg,¹⁹ T. Ogawa,⁵⁴ S. Oh,¹² Y.D. Oh,²⁵ T. Ohsugi,²⁰ R. Oishi,⁵² T. Okusawa,³⁷ R. Oldeman,⁴⁰ R. Orava,¹⁹ W. Orejudos,²⁶ C. Pagliarone,⁴¹ F. Palmonari,⁴¹ R. Paoletti,⁴¹ V. Papadimitriou,⁴⁹ D. Partos,⁴ S. Pashapour,⁵⁰ J. Patrick,¹³ G. Pauletta,⁵¹ M. Paulini,⁹ T. Pauly,³⁸ C. Paus,²⁹ D. Pellett,⁵ A. Penzo,⁵¹ T.J. Phillips,¹² G. Piacentino,⁴¹ J. Piedra,⁸ K.T. Pitts,²¹ A. Pompos,⁴³ L. Pondrom,⁵⁵ G. Pope,⁴² O. Poukhov,¹¹ F. Prakoshyn,¹¹ T. Pratt,²⁷ A. Pronko,¹⁴ J. Proudfoot,² F. Ptohos,¹⁵ G. Punzi,⁴¹ J. Rademacker,³⁸ A. Rakitine,²⁹ S. Rappoccio,¹⁸ F. Ratnikov,⁴⁷ H. Ray,³⁰ A. Reichold,³⁸ V. Rekovic,³³ P. Renton,³⁸ M. Rescigno,⁴⁶ F. Rimondi,³ K. Rinnert,²³ L. Ristori,⁴¹ M. Riveline,⁵⁰ W.J. Robertson,¹² A. Robson,³⁸ T. Rodrigo,⁸ S. Rolli,⁵³ L. Rosenson,²⁹ R. Roser,¹³ R. Rossin,³⁹ C. Rott,⁴³ J. Russ,⁹ A. Ruiz,⁸ D. Ryan,⁵³ H. Saarikko,¹⁹ A. Safonov,⁵ R. St. Denis,¹⁷ W.K. Sakumoto,⁴⁴ D. Saltzberg,⁶ C. Sanchez,³⁵ A. Sansoni,¹⁵ L. Santi,⁵¹ S. Sarkar,⁴⁶ K. Sato,⁵² P. Savard,⁵⁰ A. Savoy-Navarro,¹³ P. Schemitz,²³ P. Schlabach,¹³ E.E. Schmidt,¹³ M.P. Schmidt,⁵⁶ M. Schmitt,³⁴ G. Schofield,⁵ L. Scodellaro,³⁹ A. Scribano,⁴¹ F. Scuri,⁴¹ A. Sedov,⁴³ S. Seidel,³³ Y. Seiya,⁵² F. Semeria,³ L. Sexton-Kennedy,¹³ I. Sfiligoi,¹⁵ M.D. Shapiro,²⁶ T. Shears,²⁷ P.F. Shepard,⁴² M. Shimojima,⁵² M. Shochet,¹⁰ Y. Shon,⁵⁵ A. Sidoti,⁴¹ M. Siket,¹ A. Sill,⁴⁹ P. Sinervo,⁵⁰ A. Sisakyan,¹¹ A. Skiba,²³ A.J. Slaughter,¹³ K. Sliwa,⁵³ J.R. Smith,⁵ F.D. Snider,¹³ R. Snihur,²⁸ S.V. Somalwar,⁴⁷ J. Spalding,¹³ M. Spezziga,⁴⁹ L. Spiegel,¹³ F. Spinella,⁴¹ M. Spiropulu,¹⁰ H. Stadie,²³ B. Stelzer,⁵⁰ O. Stelzer-Chilton,⁵⁰ J. Strologas,²¹ D. Stuart,⁷ A. Sukhanov,¹⁴ K. Sumorok,²⁹ H. Sun,⁵³ T. Suzuki,⁵² A. Taffard,²¹ S.F. Takach,³⁰ H. Takano,⁵² R. Takashima,²⁰ Y. Takeuchi,⁵² K. Takikawa,⁵² P. Tamburello,¹² M. Tanaka,² R. Tanaka,³⁶ B. Tannenbaum,⁶ N. Tanimoto,³⁶ S. Tapprogge,¹⁹ M. Tecchio,³⁰ P.K. Teng,¹ K. Terashi,⁴⁵ R.J. Tesarek,¹³ S. Tether,²⁹ J. Thom,¹³ A.S. Thompson,¹⁷ E. Thomson,³⁵ R. Thurman-Keup,² P. Tipton,⁴⁴ V. Tiwari,⁹ S. Tkaczyk,¹³ D. Toback,⁴⁸ K. Tollefson,³¹ D. Tonelli,⁴¹ M. Tönnesmann,³¹ S. Torre,⁴¹ D. Torretta,¹³ W. Trischuk,⁵⁰ J. Tseng,²⁹ R. Tsuchiya,⁵⁴ S. Tsuno,⁵² D. Tsybychev,¹⁴ N. Turini,⁴¹ M. Turner,²⁷ F. Ukegawa,⁵² T. Unverhau,¹⁷ S. Uozumi,⁵² D. Usynin,⁴⁰ L. Vacavant,²⁶ T. Vaiciulis,⁴⁴ A. Varganov,³⁰ E. Vataga,⁴¹ S. Vejcik III,¹³ G. Velev,¹³ G. Veramendi,²⁶ T. Vickey,²¹ R. Vidal,¹³ I. Vila,⁸ R. Vilar,⁸ I. Volobouev,²⁶ M. von der Mey,⁶ R. G. Wagner,² R. L. Wagner,¹³ W. Wagner,²³ N. Wallace,⁴⁷ T. Walter,²³ Z. Wan,⁴⁷ M.J. Wang,¹ S.M. Wang,¹⁴ B. Ward,¹⁷ S. Waschke,¹⁷ D. Waters,²⁸ T. Watts,⁴⁷ M. Weber,²⁶

W. Wester,¹³ B. Whitehouse,⁵³ A.B. Wicklund,² E. Wicklund,¹³ T. Wilkes,⁵ H.H. Williams,⁴⁰ P. Wilson,¹³ B.L. Winer,³⁵ P. Wittich,⁴⁰ S. Wolbers,¹³ M. Wolter,⁵³ M. Worcester,⁶ S. Worm,⁴⁷ T. Wright,³⁰ X. Wu,¹⁶ F. Würthwein,²⁹ A. Wyatt,²⁸ A. Yagil,¹³ T. Yamashita,³⁶ K. Yamamoto,³⁷ U.K. Yang,¹⁰ W. Yao,²⁶ G.P. Yeh,¹³ K. Yi,²² J. Yoh,¹³ P. Yoon,⁴⁴ K. Yorita,⁵⁴ T. Yoshida,³⁷ I. Yu,²⁵ S. Yu,⁴⁰ Z. Yu,⁵⁶ J.C. Yun,¹³ L. Zanello,⁴⁶ A. Zanetti,⁵¹ I. Zaw,¹⁸ F. Zetti,⁴¹ J. Zhou,⁴⁷ A. Zsenei,¹⁶ and S. Zucchelli,³

(CDF Collaboration)

¹ *Institute of Physics, Academia Sinica, Taipei, Taiwan 11529, Republic of China*

² *Argonne National Laboratory, Argonne, Illinois 60439*

³ *Istituto Nazionale di Fisica Nucleare, University of Bologna, I-40127 Bologna, Italy*

⁴ *Brandeis University, Waltham, Massachusetts 02254*

⁵ *University of California at Davis, Davis, California 95616*

⁶ *University of California at Los Angeles, Los Angeles, California 90024*

⁷ *University of California at Santa Barbara, Santa Barbara, California 93106*

⁸ *Instituto de Fisica de Cantabria, CSIC-University of Cantabria, 39005 Santander, Spain*

⁹ *Carnegie Mellon University, Pittsburgh, Pennsylvania 15213*

¹⁰ *Enrico Fermi Institute, University of Chicago, Chicago, Illinois 60637*

¹¹ *Joint Institute for Nuclear Research, RU-141980 Dubna, Russia*

¹² *Duke University, Durham, North Carolina 27708*

¹³ *Fermi National Accelerator Laboratory, Batavia, Illinois 60510*

¹⁴ *University of Florida, Gainesville, Florida 32611*

¹⁵ *Laboratori Nazionali di Frascati, Istituto Nazionale di Fisica Nucleare, I-00044 Frascati, Italy*

¹⁶ *University of Geneva, CH-1211 Geneva 4, Switzerland*

¹⁷ *Glasgow University, Glasgow G12 8QQ, United Kingdom*

¹⁸ *Harvard University, Cambridge, Massachusetts 02138*

¹⁹ *The Helsinki Group: Helsinki Institute of Physics; and Division of High Energy Physics, Department of Physical Sciences, University of Helsinki, FIN-00014 Helsinki, Finland*

²⁰ *Hiroshima University, Higashi-Hiroshima 724, Japan*

²¹ *University of Illinois, Urbana, Illinois 61801*

²² *The Johns Hopkins University, Baltimore, Maryland 21218*

- ²³ Institut für Experimentelle Kernphysik, Universität Karlsruhe, 76128 Karlsruhe, Germany
- ²⁴ High Energy Accelerator Research Organization (KEK), Tsukuba, Ibaraki 305, Japan
- ²⁵ Center for High Energy Physics: Kyungpook National University, Taegu 702-701; Seoul National University, Seoul 151-742; and SungKyunKwan University, Suwon 440-746; Korea
- ²⁶ Ernest Orlando Lawrence Berkeley National Laboratory, Berkeley, California 94720
- ²⁷ University of Liverpool, Liverpool L69 7ZE, United Kingdom
- ²⁸ University College London, London WC1E 6BT, United Kingdom
- ²⁹ Massachusetts Institute of Technology, Cambridge, Massachusetts 02139
- ³⁰ University of Michigan, Ann Arbor, Michigan 48109
- ³¹ Michigan State University, East Lansing, Michigan 48824
- ³² Institution for Theoretical and Experimental Physics, ITEP, Moscow 117259, Russia
- ³³ University of New Mexico, Albuquerque, New Mexico 87131
- ³⁴ Northwestern University, Evanston, Illinois 60208
- ³⁵ The Ohio State University, Columbus, Ohio 43210
- ³⁶ Okayama University, Okayama 700-8530, Japan
- ³⁷ Osaka City University, Osaka 588, Japan
- ³⁸ University of Oxford, Oxford OX1 3RH, United Kingdom
- ³⁹ Università di Padova, Istituto Nazionale di Fisica Nucleare, Sezione di Padova-Trento, I-35131 Padova, Italy
- ⁴⁰ University of Pennsylvania, Philadelphia, Pennsylvania 19104
- ⁴¹ Istituto Nazionale di Fisica Nucleare, University and Scuola Normale Superiore of Pisa, I-56100 Pisa, Italy
- ⁴² University of Pittsburgh, Pittsburgh, Pennsylvania 15260
- ⁴³ Purdue University, West Lafayette, Indiana 47907
- ⁴⁴ University of Rochester, Rochester, New York 14627
- ⁴⁵ The Rockefeller University, New York, New York 10021
- ⁴⁶ Instituto Nazionale de Fisica Nucleare, Sezione di Roma, University di Roma I, "La Sapienza," I-00185 Roma, Italy
- ⁴⁷ Rutgers University, Piscataway, New Jersey 08855
- ⁴⁸ Texas A&M University, College Station, Texas 77843
- ⁴⁹ Texas Tech University, Lubbock, Texas 79409
- ⁵⁰ Institute of Particle Physics, University of Toronto, Toronto M5S 1A7, Canada
- ⁵¹ Istituto Nazionale di Fisica Nucleare, Universities of Trieste and Udine, Italy
- ⁵² University of Tsukuba, Tsukuba, Ibaraki 305, Japan
- ⁵³ Tufts University, Medford, Massachusetts 02155

⁵⁴ *Waseda University, Tokyo 169, Japan*

⁵⁵ *University of Wisconsin, Madison, Wisconsin 53706*

⁵⁶ *Yale University, New Haven, Connecticut 06520*

We report on a search for the flavor-changing neutral current decay $D^0 \rightarrow \mu^+ \mu^-$ in $p\bar{p}$ collisions at $\sqrt{s}=1.96$ TeV using 65 pb^{-1} of data collected by the CDF II experiment at the Fermilab Tevatron Collider. A displaced-track trigger selects long-lived D^0 candidates in the $D^0 \rightarrow \mu^+ \mu^-$ search channel, the kinematically similar $D^0 \rightarrow \pi^+ \pi^-$ channel used for normalization, the Cabibbo-favored $D^0 \rightarrow K^- \pi^+$ channel used to optimize the selection criteria in an unbiased manner, and their charge conjugates. Finding no signal events in the $D^0 \rightarrow \mu^+ \mu^-$ search window, we set an upper limit on the branching fraction $\mathcal{B}(D^0 \rightarrow \mu^+ \mu^-) \leq 2.5 \times 10^{-6}$ (3.3×10^{-6}) at the 90% (95%) confidence level.

PACS numbers: 13.20.Fc, 14.40.Lb

The flavor-changing neutral current (FCNC) decay $D^0 \rightarrow \mu^+ \mu^-$ [1] is highly suppressed in the Standard Model (SM) by the nearly exact Glashow-Iliopoulos-Maiani (GIM) [2] cancellation. Observation of this decay at a rate significantly exceeding the SM expectation would indicate the presence of non-SM particles or couplings. In the context of the SM, Burdman *et al.* [3] calculate the branching fraction to be $\mathcal{B}(D^0 \rightarrow \mu^+ \mu^-) \approx 10^{-18}$ from short-distance processes, increasing to $\mathcal{B}(D^0 \rightarrow \mu^+ \mu^-) \approx 10^{-13}$ when long-distance processes are included. This prediction is many orders of magnitude beyond the reach of the present generation of experiments, whose most stringent published limits are 4.1×10^{-6} from BEATRICE [4] and 4.2×10^{-6} from E771 [5] at the 90% confidence level. Thus, a large, unexplored region exists in which to search for new physics.

Burdman *et al.* consider the effects on $D^0 \rightarrow \mu^+ \mu^-$ from a number of extensions to the Standard Model: R-parity violating SUSY, multiple Higgs doublets, extra fermions, extra dimensions, and extended technicolor. They find that the $D^0 \rightarrow \mu^+ \mu^-$ branching ratio can be enhanced by orders of magnitude to the range of 10^{-8} to 10^{-10} in these scenarios, and in the case of R-parity violating SUSY, roughly to the level of the existing experimental limit. Similar enhancements can occur in K and B -decays, but charm decays provide a unique laboratory to search for new physics couplings in the up-quark sector.

This search uses a 65 pb^{-1} data sample recorded by the upgraded Collider Detector at Fermilab (CDF II) at the Tevatron $p\bar{p}$ collider with $\sqrt{s} = 1.96\text{ TeV}$ between February 2002 and January 2003. The components of the CDF II detector pertinent to this analysis are described briefly below. Detailed descriptions can be found elsewhere [6]. CDF uses a cylindrical coordinate system in which ϕ is the azimuthal angle, r is the radius from the nominal beamline, and z points in the proton beam direction and is zero at the center of the detector. The transverse plane is the plane perpendicular to the z axis. The pseudorapidity η is defined as $\eta \equiv \tanh^{-1}(\cos\theta)$, where θ is the polar angle measured from the z axis. A silicon microstrip detector (SVX II) [7] and a cylindrical drift chamber (COT) [8] immersed in a 1.4 T solenoidal magnetic field track charged particles in the range $|\eta| < 1.0$. The SVX II provides up to five $r\text{-}\phi$ position measurements, each of roughly $15\text{ }\mu\text{m}$ precision, at radii between 2.5 and 10.6 cm. The COT has 96 measurement layers, between 40 cm and 137 cm in radius, organized into alternating axial and $\pm 2^\circ$ stereo superlayers. The solenoid covers $r < 150\text{ cm}$, and electromagnetic and hadronic calorimetry occupy the region between 150 and 350 cm in radius. Four layers of planar drift chambers (CMU) [9] outside the hadron calorimeter cover the region $|\eta| < 0.6$ and detect muons of transverse momentum $p_T > 1.4\text{ GeV}/c$ penetrating the 5 absorption lengths of calorimeter material.

The D^0 decays used in this analysis are selected with a three-level trigger system. At the first level, charged tracks are reconstructed in the COT transverse plane by a hardware processor (XFT) [10]. The trigger requires two oppositely charged tracks with reconstructed transverse momenta $p_T \geq 2\text{ GeV}/c$ and $p_{T1} + p_{T2} \geq 5.5\text{ GeV}/c$. At the second level, the Silicon Vertex Tracker (SVT) [11] associates SVX II position measurements with XFT tracks. The impact parameter of the track, d_0 , with respect to the beamline, is measured with $50\text{ }\mu\text{m}$ resolution, which includes a $\sim 30\text{ }\mu\text{m}$ contribution from the transverse beam size. Requiring two tracks with $120\text{ }\mu\text{m} \leq |d_0| \leq 1.0\text{ mm}$ selects a sample enriched in heavy flavor. The two trigger tracks must have an opening angle satisfying $2^\circ \leq |\Delta\phi| \leq 90^\circ$ and be consistent with the decay of a particle traveling a transverse distance $L_{xy} > 200\text{ }\mu\text{m}$ from the beamline. At the third level, a computing farm performs complete event reconstruction. The sample of $\sim 10^5$ D^* -tagged two-body D^0 decays selected by the trigger is used to estimate backgrounds, to optimize selection requirements, and to normalize the sensitivity of the search from the data sample itself.

The $D^0 \rightarrow \mu^+ \mu^-$ branching ratio, or upper limit, is determined using

$$\mathcal{B}(D^0 \rightarrow \mu^+ \mu^-) \leq \mathcal{B}(D^0 \rightarrow \pi^+ \pi^-) \frac{N(\mu\mu)}{N(\pi\pi)} \frac{\epsilon(\pi\pi)}{\epsilon(\mu\mu)} \frac{a(\pi\pi)}{a(\mu\mu)}, \quad (1)$$

where $\mathcal{B}(D^0 \rightarrow \pi^+ \pi^-) = (1.43 \pm 0.07) \times 10^{-3}$ is the measured normalization branching fraction [12], $N(\mu\mu)$ and $N(\pi\pi)$ are the numbers of $D^0 \rightarrow \mu^+ \mu^-$ and $D^0 \rightarrow \pi^+ \pi^-$ events observed, and ϵ and a are the efficiency and acceptance for each mode. Except for the requirement of muon identification, and the assignment of different particle masses, the same selection requirements are applied to both modes. In this analysis, we determined the upper limit on the number of signal events observed, $N(\mu\mu)$, by assuming that the number of events found in the signal region is the sum of signal and background events, both obeying Poisson statistics. Normalization was made to $D^0 \rightarrow \pi^+ \pi^-$ rather than the more numerous $D^0 \rightarrow K^- \pi^+$ decays. Kinematically, the $D^0 \rightarrow \pi^+ \pi^-$ mode is nearly identical to $D^0 \rightarrow \mu^+ \mu^-$, minimizing the differences in acceptance and efficiency, and introducing minimal systematic uncertainty to the result. The width of the reconstructed mass peak for two-body decays of the D^0 in CDF II is about $10 \text{ MeV}/c^2$, sufficient to separate $D^0 \rightarrow K^- \pi^+$ kinematically from $D^0 \rightarrow \pi^+ \pi^-$ (Fig. 1).

In the spirit of obtaining an unbiased result, a “blinded” analysis was performed. The data in the signal mass window were hidden and the analysis cuts optimized without knowledge of their actual impact on the result. The optimization was performed on kinematically similar but statistically independent events. Only after all selection criteria had been fixed was the signal region “unblinded” and the final result determined.

We first outline the general event selection requirements common to all the data samples used in the analysis and then discuss how they are used to determine the quantities in Eq. (1). All of the samples consist of $D^{*+} \rightarrow D^0 \pi^+$ candidate decays coming from data sets where all requisite detector components were functioning properly, specifically, the SVX, COT, and CMU detectors, and the displaced-track trigger chain. D^0 candidates were formed from pairs of oppositely charged “trigger tracks” that are “CMU fiducial”. Trigger tracks are tracks reconstructed offline that have been matched to online SVT tracks. A track that intercepts the active region of the CMU when extrapolated from the COT through the magnetic field of the detector is said to be CMU fiducial.

To select D^0 candidates in a given decay mode, $K^+ \pi^-$, $\pi^+ \pi^-$, or $\mu^+ \mu^-$, we evaluated the invariant mass of each pair of trigger tracks using the corresponding mass assignment

and kept candidates in the range $1.840 \text{ GeV}/c^2 < M_{\text{pair}} < 1.884 \text{ GeV}/c^2$. This corresponds to slightly more than $\pm 2\sigma$ around the mean of the D^0 mass peak, $1.862 \text{ GeV}/c^2$. The D^* tag reduces non- D^0 backgrounds and eliminates the mass peak in the $K\pi$ channel due to mis-assignment of the K and π masses. $D^{*+} \rightarrow D^0\pi_s^+$ decays were selected by combining an additional pion track (π_s) with the D^0 candidate and requiring the mass difference $M_{\text{pair}+\pi_s} - M_{\text{pair}}$ to lie in the range $144 \text{ MeV}/c^2$ to $147 \text{ MeV}/c^2$. The π_s track was not required to be CMU fiducial or to be a trigger track, but it had to have the Cabibbo-favored charge for the $K\pi$ decay.

The ratio $\epsilon(\pi\pi)/\epsilon(\mu\mu)$ was determined from the muon identification efficiency and the pion reconstruction efficiency, measured in other analyses, as follows. From a sample of $J/\psi \rightarrow \mu^+\mu^-$ decays collected by a trigger requiring one identified muon and one SVT track, the CMU identification efficiency for the unbiased muon was measured offline as a function of its transverse momentum p_T . We convoluted the efficiency spectrum with the p_T spectrum of pions from $D^0 \rightarrow \pi^+\pi^-$ and determined the effective dimuon identification efficiency to be $\epsilon(\mu\mu) = 0.800 \pm 0.030$. Using a detailed GEANT [13] detector simulation, the pion reconstruction efficiency was found to be $95 \pm 1\%$, yielding $\epsilon(\pi\pi) = 0.90 \pm 0.02$, where the inefficiency arises primarily from hadronic interactions with detector material. Combining these values we find $\epsilon(\pi\pi)/\epsilon(\mu\mu) = 1.13 \pm 0.04$. Using the same detector simulation, we find the acceptance ratio $a(\pi\pi)/a(\mu\mu) = 0.96 \pm 0.02$.

The number of $D^0 \rightarrow \pi^+\pi^-$ decays, $N(\pi\pi)$, was determined by fitting the peak in the $\pi\pi$ invariant mass spectrum. We performed a binned χ^2 fit with Gaussian signal plus linear background, as shown in Fig. 1. Both the mean and width of the Gaussian were free parameters in the fit. $N(\pi\pi)$ is the integral of the Gaussian over the $\pm 22 \text{ MeV}/c^2$ mass window around $1.862 \text{ GeV}/c^2$.

The background to $D^0 \rightarrow \mu^+\mu^-$ was taken as the sum of two contributions having different mass spectra: a peaked contribution from $D^0 \rightarrow \pi^+\pi^-$ decays in which both pions are misidentified as muons, and a relatively flat background due to all other sources. The flat background was estimated from the number of $\mu\mu$ candidates in a high mass sideband spanning the range $1.90 \text{ GeV}/c^2 < M_{\mu\mu} < 2.05 \text{ GeV}/c^2$ with both tracks identified as muons. Before muon identification of the tracks is required, the distribution of events in the high mass sideband is found to be roughly constant, and we assume that this remains true after requiring muon identification. The expected flat background is the number of sideband

events scaled by the ratio of the width of the signal region to the sideband region, 44/150.

The misidentification background was estimated from the number of $D^0 \rightarrow \pi^+\pi^-$ events reconstructed with the $\mu\mu$ mass assignment and lying in the $\pm 22 \text{ MeV}/c^2$ signal window (shaded area falling between the arrows in Fig. 1) times the square of the probability for a pion to be misidentified as a muon. The π -misidentification probability was determined from the sample of D^* -tagged $D^0 \rightarrow K^-\pi^+$ events. The average π -misidentification probability is $1.3 \pm 0.1\%$.

Three additional selection requirements were imposed. To remove instances in which the two D^0 decay daughters extrapolate to the same region of the CMU, potentially correlating the muon identification of the two tracks, we cut on the azimuthal angle $\Delta\phi_{CMU}$ between their projections into the CMU. To suppress combinatoric backgrounds, we cut on the impact parameter with respect to the beamline, d_{xy} , of the reconstructed D^0 trajectory. Further, we cut on the transverse decay length of the D^0 candidate, L_{xy} . The values of these cuts were optimized as described below.

We determined the optimal cut values by maximizing a figure of merit given by $S/(1.5 + \sqrt{B})$ [14] where S and B represent the number of signal and background events, respectively. This quantity has desirable properties for an analysis where both the signal and background are small: it behaves as S/\sqrt{B} for large B and it behaves as S as the estimated background approaches zero. The constant in the denominator is chosen to favor cuts that maximize the discovery reach at 3σ significance. To estimate S in the optimization, we used the $D^0 \rightarrow \pi^+\pi^-$ sample. To estimate the misidentification component of B , we used a sample of $D^0 \rightarrow K^-\pi^+$ decays in which both tracks were found to be misidentified as muons. To estimate all remaining contributions to B , we used the subset of the high-mass $\pi\pi$ sideband sample in which one track was identified as a muon and the other was not. Note that the events used to estimate B in the optimization are distinct from the events used in the final background estimate for the result. The resulting selection requirements are: $|\Delta\phi_{CMU}| > 0.085 \text{ rad}$, $|d_{xy}| < 150 \mu\text{m}$, and $L_{xy} < 0.45 \text{ cm}$. When applied to the samples used for optimization these cuts remove approximately 58% of the background events and 12% of the signal events.

Using the optimized selection requirements, 5.0 ± 2.2 events remain in the high mass sideband, yielding 1.6 ± 0.7 expected from the flat component of the background. The number of $D^0 \rightarrow \pi^+\pi^-$ events falling in the signal window when reconstructed using the

muon mass, multiplied by the square of the 1.3% π -misidentification probability, yields 0.22 ± 0.02 expected misidentification events. The total expected background is 1.8 ± 0.7 events. The number of events in the normalization mode is $N(\pi\pi) = 1412 \pm 54$ (Fig. 1). Using this background estimate and normalization, the 90% confidence level sensitivity [15] is 4.4×10^{-6} .

We apply the optimized selection requirements to the signal region of the $\mu\mu$ sample and find no events remaining, as displayed in Fig. 2. Conservatively taking the number of background events to equal zero, the 90% (95%) confidence level upper limit on the number of $D^0 \rightarrow \mu^+ \mu^-$ events is 2.3 (3.0). Using Eq. (1) we find an upper limit on the branching fraction of $\mathcal{B}(D^0 \rightarrow \mu^+ \mu^-) \leq 2.5 \times 10^{-6} (3.3 \times 10^{-6})$ at the 90% (95%) confidence level.

The uncertainties on $N(\pi\pi)$, $\epsilon(\pi\pi)/\epsilon(\mu\mu)$, $a(\pi\pi)/a(\mu\mu)$, and $\mathcal{B}(D^0 \rightarrow \pi^+ \pi^-)$ are incorporated into the limit using the prescription of Cousins and Highland [16]. However, all of the uncertainties are smaller than 5% and have a negligible effect on the limit.

In summary, we have searched for the FCNC decay $D^0 \rightarrow \mu^+ \mu^-$, using the new displaced-track trigger of the CDF II experiment. This is the first result from CDF in the field of rare charm decays. To minimize bias in the event selection, a blinded search was performed. To minimize dependence on Monte Carlo simulation, most of the needed quantities were determined directly from the data. No events were observed and we set an upper limit on the branching ratio of

$$\mathcal{B}(D^0 \rightarrow \mu^+ \mu^-) \leq 2.5 \times 10^{-6} (3.3 \times 10^{-6}) \quad (2)$$

at the 90% (95%) confidence level. This result improves on the best limits published to date.

Acknowledgments

We thank the Fermilab staff and the technical staffs of the participating institutions for their vital contributions. This work was supported by the U.S. Department of Energy and National Science Foundation; the Italian Istituto Nazionale di Fisica Nucleare; the Ministry of Education, Culture, Sports, Science and Technology of Japan; the Natural Sciences and Engineering Research Council of Canada; the National Science Council of the Republic of China; the Swiss National Science Foundation; the A.P. Sloan Foundation; the Bundesministerium fuer Bildung and Forschung, Germany; the Korean Science and

Engineering Foundation and the Korean Research Foundation; the Particle Physics and Astronomy Research Council and the Royal Society, UK; the Russian Foundation for Basic Research; and the Comision Interministerial de Ciencia y Tecnologia, Spain.

- [1] Throughout this paper inclusion of charge conjugate modes is implicit.
- [2] S.L. Glashow, J. Iliopoulos, and L. Maiani, Phys. Rev. **D2**, 1285 (1970).
- [3] G. Burdman, E. Golowich, J. Hewett, and S. Pakvasa, Phys. Rev. **D66**, 014009 (2002).
- [4] M. Adamovich *et al.* (BEATRICE), Phys. Lett. **B408**, 469 (1997).
- [5] T. Alexopoulos *et al.* (E771), Phys. Rev. Lett. **77**, 2380 (1996).
- [6] R. Blair *et al.*, FERMILAB-PUB-96/390-E (1996).
- [7] A. Sill *et al.*, Nucl. Instrum. Meth. **A 447**, 1 (2000).
- [8] K.T. Pitts *et al.*, Nucl. Phys. Proc. Suppl. **61B**, 230 (1998).
- [9] F. Abe *et al.*, Nucl. Instrum. Methods **A 271**, 387 (1988); F. Abe *et al.*, Phys. Rev. **D50**, 2966 (1994).
- [10] E.J. Thomson *et al.*, IEEE Trans. Nucl. Sci. **49**, 1063 (2002).
- [11] W. Ashmanskas *et al.*, Nucl. Instrum. Meth. **A 447**, 218 (2000); W. Ashmanskas *et al.*, Report no. FERMILAB-CONF-03/168-E.
- [12] K. Hagiwara *et al.*, Phys. Rev. **D66**, 010001 (2002).
- [13] R. Brun, R. Hagelberg, M. Hansroul, and J.C. Lassalle, Reports no. CERN-DD-78-2-REV and CERN-DD-78-2.
- [14] G. Punzi, physics/0308063, August 2003.
- [15] G.J. Feldman and R.D. Cousins, Phys. Rev. **D57**, 3873 (1998).
- [16] R.D. Cousins and V.L. Highland, Nucl. Instrum. Meth. **A320**, 331 (1992).

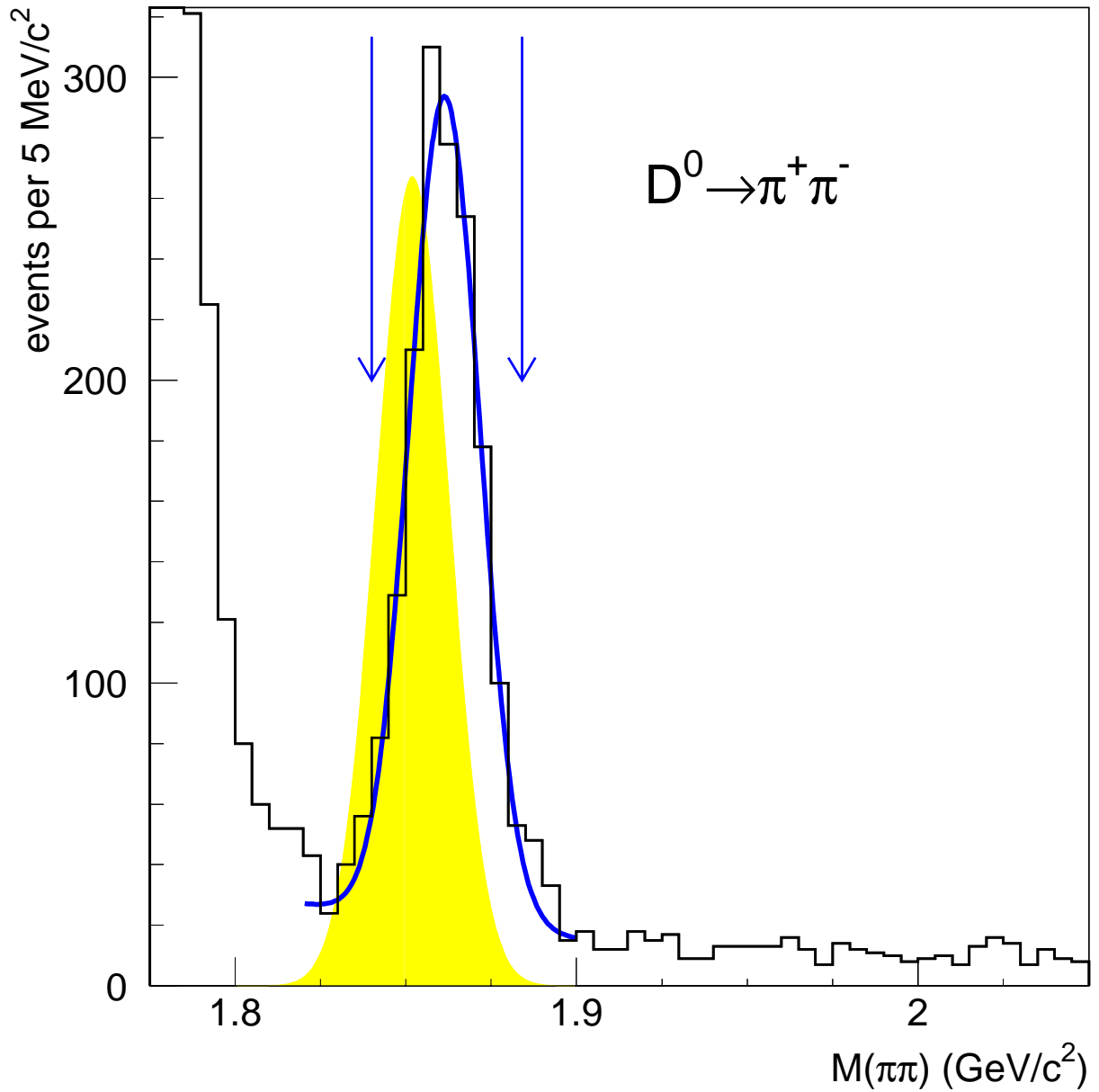


FIG. 1: The mass distribution of candidate $D^0 \rightarrow \pi^+\pi^-$ events. The $D^0 \rightarrow \mu^+\mu^-$ branching ratio was normalized to the kinematically similar mode $D^0 \rightarrow \pi^+\pi^-$. The arrows indicate the $\pm 22 \text{ MeV}/c^2$ mass window used for the signal. The curve is a fit over the range 1.82 to $1.90 \text{ GeV}/c^2$ with Gaussian signal plus linear background. The shaded Gaussian represents the effect of reconstructing the events with a $\mu^+\mu^-$ mass assignment. The large $K\pi$ signal below $1.82 \text{ GeV}/c^2$ is kinematically separate from the region of interest. The distribution of events in the region above the D^0 mass is roughly flat.

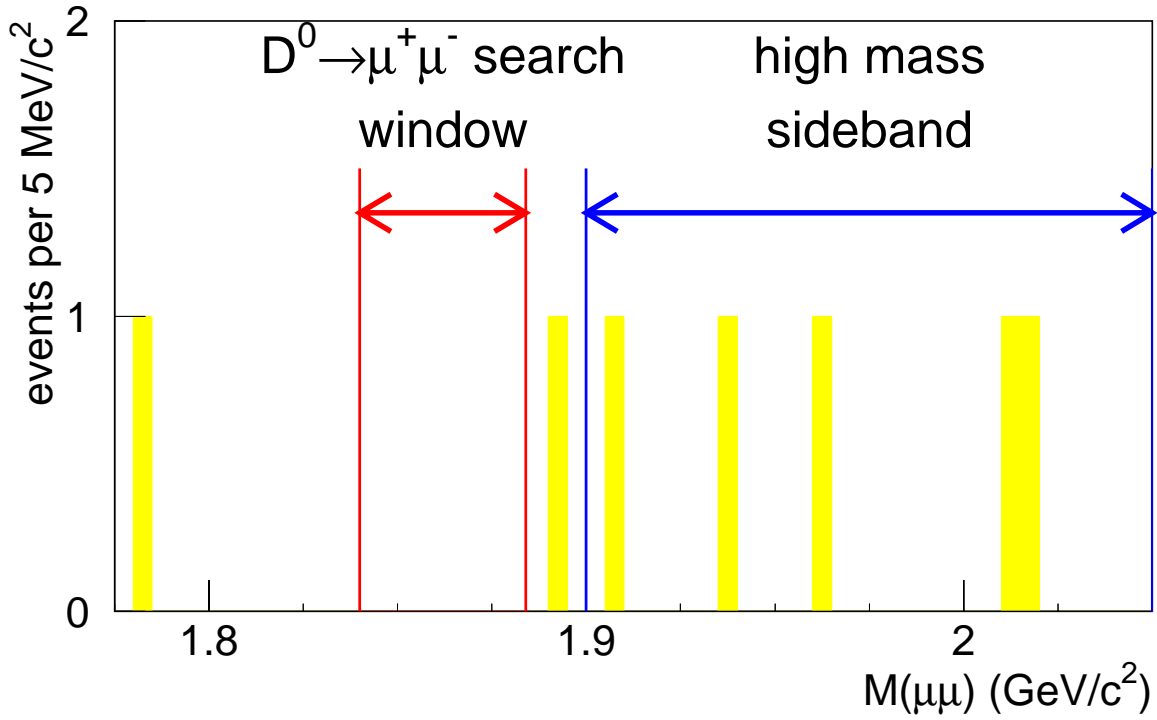


FIG. 2: The mass distribution of candidate $D^0 \rightarrow \mu^+ \mu^-$ events. No events remain in the D^0 mass region satisfying the event requirements. The events in the high mass sideband were used to estimate the background from all sources other than misidentification of $D^0 \rightarrow \pi^+ \pi^-$.